Available online on 15.07.2019 at http://jddtonline.info

Journal of Drug Delivery and Therapeutics

Open Access to Pharmaceutical and Medical Research

© 2011-18, publisher and licensee JDDT, This is an Open Access article which permits unrestricted non-commercial use, provided the original work is properly cited

Open Access Research Article

Demonstration of Lymphatic Uptake of (6)-Gingerol Solid Lipid Nanoparticles

Dr. Mangesh R Bhalekar*[1], Dr. Ashwini Madgulkar[2], Tejaswini Jagtap[3],

[1,2,3]Department of pharmaceutics, AISSMS College of Pharmacy, Savitribai Phule Pune University, Pune, India-411001

ABSTRACT

(6)-Gingerol, a disease modifying anti-rheumatoid drug (DMARD) agent in the treatment of Rheumatoid Arthritis is a potent inhibitor of COX-1, COX-2 activity, inhibits PGE2 production. It also inhibits the production of TNF-α by blocking the cell associated conversion of TNF precursor to mature proteins thus, halting the proliferation of synovitis. (6)-Gingerol undergo extensive phase I metabolism & underlies low systemic exposure. The aim of the present study was to overcome these limitations and formulate and evaluate Ginger extract Solid Lipid Nanoparticles to improve bioavailability by enabling lymphatic uptake. (6)-Gingerol Solid Lipid Nanoparticles were prepared by melt emulsification-homogenization method and the particle size, Zeta potential PDI and % entrapment efficiency was optimized using Box Behnken design. The optimized SLN were found to be 237nm in size, bearing -25.3mv zeta potential, 0.350 PDI and entrapment efficiency of 91.33%. *Ex vivo* endocytic uptake studies (everted intestine method) revealed involvement of endocytic pathways in the uptake of Solid Lipid Nanoparticles from intestine. Thus underlining the utility of SLN for enhancement of uptake of (6)-Gingerol.

Keywords: (6)-Gingerol; Stearic acid; Solid lipid nanoparticles; High pressure homogenization; Lymphatic uptake; Rheumatoid arthritis.

Article Info: Received 19 May 2019; Review Completed 25 June 2019; Accepted 05 July 2019; Available online 15 July 2019

Cite this article as:

Bhalekar MR, Dr. Madgulkar A, Jagtap T, Demonstration of Lymphatic Uptake of (6)-Gingerol Solid Lipid Nanoparticles, Journal of Drug Delivery and Therapeutics. 2019; 9(4):461-469 **http://dx.doi.org/10.22270/jddt.v9i4.3193**

***Address for Correspondence:**

Dr. Mangesh R Bhalekar, Professor, AISSMS College of Pharmacy, Savitribai Phule Pune University, Pune-411001. India.

ABBREVIATIONS: DMARD- Disease Modifying Anti-Rheumatoid Drug, SLN-Solid ipid nanoparticles, EE -Entrapment efficiency.

1. INTRODUCTION

The traditional approach to treatment of rheumatoid arthritis (RA) is a combination of disease modifying anti rheumatoid drugs (DMARDs) and NSAIDs [1]. Various agents such as chloroquine, 5fluoro uracil, sulfasalazine have been reported to have disease modifying properties[1,2,3]. However the toxicity of some of these agents leads us to look to phytochemicals which have DMARD like action, there are many medicinal plant extracts that have been shown to be effective in treating RA, e.g. aloe vera, ashwagandha, ginger, piperine [4]. One such compound (6)-Gingerol($C_{17}H_{26}O_4$) is homologous phenolic ketones found in fresh ginger rhizome (Zingiber officinale Rosco) belonging to the family Zingiberaceae [8].

(6)-Gingerol inhibits the production of TNF-α by blocking the cell associated conversion of TNF Precursor to mature proteins thus halting the proliferation of synovitis. Gingerol is a potent inhibitor of COX-1, COX-2 activity and inhibits PGE2 production thus decrease proliferation of inflammation and disease condition. (6)-Gingerol is given orally in a dose of 120mg//kg/day. The low solubility of (6)-Gingerol has led to its poor oral absorption and fast metabolism has hindered the clinical applications of the drug [5,6]. Currently, gingerols are available as soft capsule formulation. It has been suggested that new therapeutic approaches should be directed at overcoming the issues relating to effective delivery, potential off-target effects, safety, toxicity, large-scale production costs, and tissue specificity [5,6].

To overcome these limitations, (6)-Gingerol has been formulated as SMEDDS and proliposomes which has resulted in improved bioavailability by 5-fold in vivo compared with free drug [5,6]. Solid Lipid Nanoparticles (SLN) are colloidal drug carriers and have particle size ranging from 50nm to 1000nm which have ability to enter lymphatic circulation when administered orally through Peyer's patch [9,10,11].

Hence formulation of (6)-Gingerol as lipid nanoparticles may be able to improve bioavailability by entry of particles through lymphatic route and also may allow the accumulation of SLN at inflamed site by passive diffusion [12].

The present work attempts to incorporate ginger extract in SLN by using principal of design of experiment (DOE) and demonstrate its lymphatic uptake by ex vivo everted rat gut sac model.

2. MATERIAL AND METHODS:

2.1. Materials

Ginger extract was obtained as a gift sample from Natural Remedies (Bangalore, India). (6)-Gingerol Marker was purchased from Sigma-Aldrich life sciences (India), Glyceryl monostearate, Compritol 888 ATO, Emulcire 61 and Precirol ATO 5 were kind gifts from Gatefosse (France). All the other chemicals and reagents were procured from local sources.

2.2 Methods

2.2.1 Standard calibration curve of (6)-Gingerol by UV-Visible Spectrophotometer

Solution of (6)-Gingerol (10 µg/ml) was in concentration range of 5 to 30µg/ml were prepared with methanol. The absorbance of resulting solutions was measured at 282 nm using double beam UV-Visible Spectrophotometer (LABINDIA UV 3000) against methanol as blank [13].

2.2.2 Selection of lipid using solubility parameter (δ) [14,15]:

Difference in the solubility parameter of drug and various lipids was considered for selection of lipid. The solubility parameter was calculated on the basis of molecular structure of the drug and lipid. The Fedors group contribution method assigns specific values to different groups as well as bonds in molecular structure and so energy of vaporization (ΔE_{υ}) and molar volume (Vm) values are specific for each group.The **δ** for each molecular structure was calculated by using the formula given below (Eq 1), and then the difference between the Solubility parameter of drug and the lipid was noted[14,15].

$$\delta = (\Delta E\upsilon/Vm)^{0.5}$$

where, ΔE_{υ} -the energy of vaporization at a given temperature and

Vm -the corresponding molar volume which is calculated from the known values of molecular weight and density.

2.2.3 Selection of Surfactant System [16]:

Melt Emulsification-homogenisation method was used to prepare SLN[18]. A mixture of Ginger extract and Stearic acid was melted at 70°C. Aqueous phase was prepared by dissolving various surfactants into distilled water at 70°C. Two phases were mixed at the same temperature followed by stirring under an over-head stirrer at 800rpm for 15 minutes to obtain a uniform emulsion, which was further subjected to High Pressure Homogeniser at homogenisation Pressure 400 bars and 9 homogenization cycles. The resultant SLN was evaluated for particle size and PDI. The surfactant system was chosen depending upon the average diameter of the globules produced and Poly Dispersity Index (PDI) of the resultant emulsion upon employing the surfactant system. (Table 1).

Table 1: Trial combinations of surfactant used for preparation of solid lipid nanoparticles.

Batches	Water Phase Surfactant (2%)
T1	Sodium Lauryl Sulphate
T2	Poloxamer 188
T3	Tween 80

2.2.4 Drug Excipient Compatibility Studies:

Compatibility of Ginger extract with Stearic acid and Tween 80 was checked in physical mixtures (1:1 ratio) stored at 40°C for two weeks. Fourier transform- infrared spectroscopic analysis (FT-IR) was carried out in Shimadzu-IR Spectrophotometer. Samples were dispersed in KBr and compressed into pellet by application of pressure. The scanning range was 4000-400 cm^{-1} and resolution was $1cm^{-1}$.

2.2.5 Optimization and formulation of SLN containing ginger extract:

A Box Behnken Design of 13 experimental runs was used to evaluate three variables at 3 levels viz. Surfactant concentration, homogenization pressure, homogenization cycle in order to determine their effect on two responses percentage entrapment efficiency and particle size and their interaction therein. The layout of the experimental design is shown in table 2 and 3.

Table 2: Design layout of box behnken design for optimization of solid lipid nanoparticles.

Sr. No.	Factors				Responses
1	Concentration of surfactant (Tween 80) (%)	-1	0	+1	Percentage Entrapment Efficiency (%)
2	Homogenization Pressure (Bar)	-1	0	+1	Particle Size (nm)
3	Homogenization Cycles (number)	-1	0	+1	

Table 3: Translation of experimental conditions into physical units for preparation of solid lipid nanoparticles containing ginger extract.

Sr. No.	Factor 1(A): Aqueous Phase Surfactant (Tween 80) (%)	Factor2(B):Homogenization Pressure (Bar)	Factor3(C):Homogenization Cycles (number)
-1	0.5	400	6
0	1	800	9
+1	1.5	1200	12

2.2.6 Characterization of SLN containing ginger extract:

2.2.6.1 Determination of Particle size [25]:

The particle size analysis of the prepared Solid Lipid Nanoparticle dispersions was performed using Malvern Zetasizer ZS 90 (Malvern Instruments, Worcestershire, UK), utilizing laser diffraction with beam length 2.40 mm, range lens of 300 RF mm, and at 14.4% obscuration. The sample was diluted with distilled water prior to the analysis. The mean diameter and the poly dispersity index of each batch were recorded.

2.2.6.2 Determination of Entrapment Efficiency [25]:

The SLN dispersion was subjected to centrifugation at 20,000 rpm (Make-Remi, Model-R4C) for 15 minutes and the supernatant was analysed for unentrapped (6)-Gingerol spectrophotometrically at 282 nm using methanol as a solvent. EE was calculated according to the equation 2.

$$EE\% = \frac{The\ amount\ of\ entrapped\ drug\ in\ SLN}{The\ amount\ of\ drug\ in\ SLN\ and\ free\ drung\ in\ dipersion} X100$$

2.2.6.3 Determination of Zeta Potential:

Zeta potential analysis was carried out using the additional electrode of Malveran Zetasizer that was used for particle size and PDI analysis. A sample of SLN was diluted with distilled water and subjected into disposable sizing cuvette for measurement at temperature of 25°C with setting of dispersant RI at 1.33 and dielectric constant of dispersant at 78.5 in triplicates.

2.2.6.4 Differential Scanning Calorimetry (DSC):

Differential scanning calorimetry (DSC) studies were carried out on (6)-Gingerol, stearic acid and SLN containing ginger extract using Mettler Toledo DSC823 *e software (Columbia, USA). Samples were accurately weighed and heated in sealed aluminium pans at a rate 10°C/min between 25 - 200°C temperature rang under nitrogen atmosphere at flow rate of 40ml/minute. Empty aluminium pan was used as a reference.

2.2.7 Ex vivo endocytic uptake study [19]:

It has been seen that there are multiple methods reported for determination of uptake of lipid based nanoparticles from an intestine. In order to study the uptake of ginger extract SLN across rat intestine, endocytic uptake study using everted rat intestine model was done. Segments of small intestine of sacrificed rat were procured, cleaned and everted using a glass rod. One end of the intestinal segment was sealed using a silk suture, while from the other open end, 1 ml of phosphate buffer of pH 6.8 was added inside and sealed using silk suture. The resultant sac was further incubated in a dispersion containing SLN. (6)-Gingerol concentration in the phosphate buffer was estimated using UV method.

The uptake mechanism of the SLN was evaluated by the intestinal cells in detail, everted gut sacs as described above were also incubated with specific endocytic inhibitors like chlorpromazine (concentration of 30 µg/ml) and nystatin (concentration of 45 µg/ml) at 37 °C for 30 mins and in (6)-Gingerol-SLN dispersions at 4 °C. After 30mins of incubation the phosphate buffer from the intestinal sacs were carefully collected in test tubes and subjected to spectrophotometric analysis.

3. RESULTS AND DISCUSSION

3.1 Standard calibration curve of (6)-Gingerol by UV-Visible Spectrophotometer

Calibration curve of (6)-Gingerol was established at λ_{max} 282nm in methanol. The Beer's law was obeyed between concentration range of 5-30µg/ml and the equation of line and R^2 was found to be y=0.039x + 0.050and 0.996 respectively (figure 1).

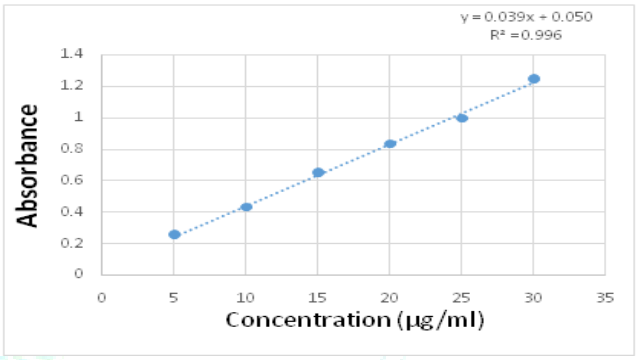


Figure 1: Calibration curve of (6)-Gingerol

3.2 Selection of Lipid Based on Solubility Parameter [14,15]:

The solubility parameter of a liquid δ, defined as the square root of the cohesive energy density is a quantity which, in conjunction with suitable theory, allows one to estimate several thermodynamic properties of solutions. The cohesive energy density itself is defined as the ratio of the energy of vaporization, ΔE_v to the molar volume both referred to the same temperature. Solubility parameters are widely used to describe the cohesive forces within materials and have been used to describe many physical properties of a material and predict interactions between materials Table 4. Fedors group contribution method of estimating solubility parameter is superior to Small's method for two reasons:

1) the contribution of a much larger number of functional groups can be evaluated, and

2) the method requires only a knowledge of the structural formula of the compounds [15].

Table 4: Solubility parameter of (6)-Gingerol and various lipids together with their differences.

Sr. No.	Drug/ Lipid Name	Solubility Parameter ($MPa^{1/2}$)	Difference with (6)-Gingerol (Δδ)
1	Gingerol-6	24.34	---
2	Compritol 888 ATO	21.26	3.08
3	GMS	18.66	5.68
4	Precirol ATO 5	21.63	2.71
5	Emulcire 61	19.27	5.07
6	Stearic Acid	22.28	2.06

3.3 Selection of Surfactant System [16,24]:

SLN containing sodium lauryl Sulphate (SLS) produced substantially smaller particle size, but owing to the toxicity profile, high poly dispersity index and associated instability of the suspending property, it was eliminated as a choice. Other excipient such as Poloxamer 188 had smaller particle size and also low poly dispersity index due to its gelation property on storage it was not selected as surfactant for further experiments. Tween 80 resulted in particle size of 299 nm and PDI of 0.350 and hence this was chosen for further studies Table 5.

Tween 80 as a long chain surfactant provides aqueous phase stability to the emulsion formed thus leading to the formation of an emulsion system of which, low particle size and PDI is functional characteristics.

Table 5: Represents various findings of different amalgamations of lipid and water based surfactant.

Batches	Solid Lipid Stearic acid(%)	Water Phase Surfactant (Tween 80) (%)	Mean *Particle Size (nm)	*PDI	Observation
B1	Stearic acid	Sodium Lauryl Sulphate	347.30	0.328	Higher Particle Size
B2		Poloxamer 188	384.37	0.280	Has Caused Gelation on storage
B3		Tween 80	269.2	0.350	Stable on Storage

***n=3 i.e. average of three readings**

3.4 Drug Excipient Compatibility Studies:

The compatibility data of with potential formulation excipients studied by FT-IR spectroscopy is presented in Figure 2. The characteristic peaks of Ginger extract are retained. The peaks were observed at (3600 cm^{-1})- Aliphatic O-H stretch, (3100 cm^{-1})- Aromatic C-H Stretch,(896 cm^{-1})-Aliphatic C-O, (1680 cm^{-1})-C=O, (1670 cm^{-1})-C=C, (1315 cm^{-1})-C-H Stretch, with only minor shifts in wave number thus suggesting that there is no interaction between the ginger extract and other excipients. Hence drug- excipients compatibility was established.

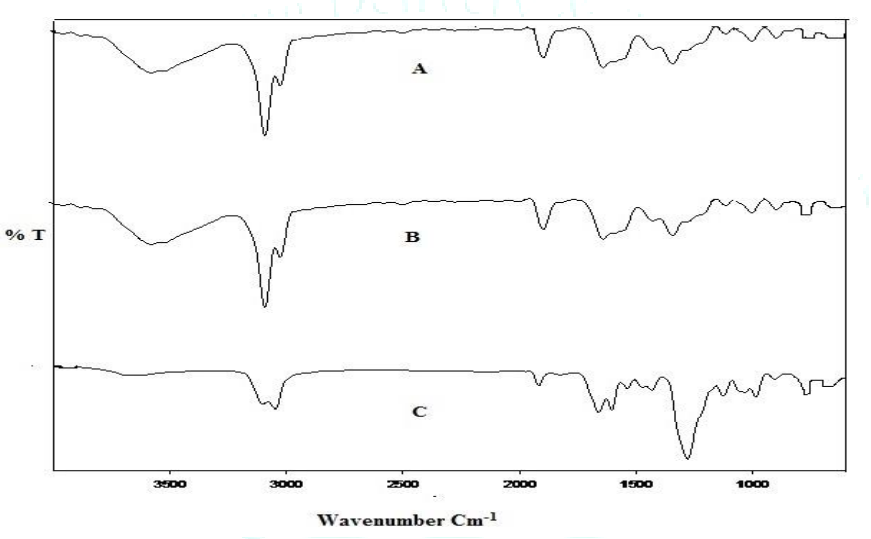


Figure 2: FT-IR spectra of (A) Ginger extract, (B) Ginger extract +Stearic Acid, (C) Ginger extract + Tween 80

3.5 Optimization and formulation of SLN containing ginger extract:

Ginger extract SLN were prepared by melt emulsification Homogenization, it is a technique in which particles are forced through a specifically engineered homogenizing valve under high density fluid-dynamic energy condition. Ginger extract SLN and Blank SLN were prepared as per the experimental design and evaluated.

The Box-Behnken design reduces number of experiments in a 3- Factor, 3-Levels experimental design from 27 to 13. Another advantage of the Box-Behnken design is that it does not contain combinations for which all factors are simultaneously screened at their highest or lowest levels.

SELECTION OF LEVELS

A) Selection of surfactant concentration:

It was observed that 0.5% concentration gives high particle size of 712 nm and when we increased the concentration of surfactant, particle size decreased upto 300. Surfactant concentration above 1.5% solubilises drug in the micelles in the aqueous phase, leading to reduce entrapment efficiency.

B) Selection of homogenization pressure:

When the applied homogenization pressure was increased from 400-1200 bar, particle size slowly decreased from 712nm to 287 nm. Homogenization pressure above 1200 bar leads to an increased particle size due to coalescence, this occurs because of the high kinetic energy of the particles [23].

C) Selection of homogenization cycles:

It was observed that as the no. of homogenization cycle increased, particle size was decreased. An increase in homogenization cycles above 12 resulted in increased particle size. This might be due to the high kinetic energy of small particles that show aggregation of particles [23].

Table 6: Experimental run and responses for optimization of ginger extract solid lipid nanoparticles formula using box- behnken design.

		Factor 1	Factor 2	Factor 3	Response 1	Response 2
Std	Run	A:Surfactant conc	B:Homogenization Pressure	C:Homogenization Cycle	Particle size	Entrapment efficiency
		%	Bar	Unit	Nm	%
7	1	0.5	800	12	570	92.16
10	2	1	1200	6	298	82.33
4	3	1.5	1200	9	230	70
5	4	0.5	800	6	584	92.25
9	5	1	400	6	681	91.25
6	6	1.5	800	6	469	80
2	7	1.5	400	9	611	80.5
12	8	0.5	1200	12	310	82.16
3	**9**	**1**	**1200**	**9**	**237**	**91.33**
11	10	1	400	12	659	90.58
8	11	1.5	800	12	447	74.58
13	12	1	800	9	510	89
1	13	0.5	400	9	712	92.33

3.6 Characterisation of SLN containing ginger extract:

3.6.1 Determination of Particle Size: The particle size across the optimization runs was observed to range between 230 to 712 nm. The particle size decreased commensurate with increasing surfactant concentration.

Equation 3 for Particle Size:

Particle Size= +510.00-51.13 A-191.00 B-8.63 C+7.75 AB-2.00 AC+2.75 BC-2.75 A^2-39.00 B^2+10.25 C^2

The proposed model for particle size indicates that term **A (conc of tween 80)** decreases particle size, as tween 80 forms a protective layer around the particle thus inhibits aggregation of particles, whereas **term B (homogenization pressure)** had most dominant effect which is due to homogenizing valve under high density fluid-dynamic energy conditions and **term C (homogenization cycle)** also contributed in decreasing particle size. All three factors are higher order term was seen to have linear relationship in reducing particle size. Similar effects were shown in figure 3, 4 and 5.

The interaction **term AB** i.e. as the surfactant concentration and homogenization pressure went on increasing it contributed to decrease the particle size. At low surfactant concentration the additional surface generated was not adequately protected by surfactant molecules and hence causing aggregation and larger particle size.

According to interaction **term AC** the particle size was seen to decrease with the increase in the surfactant concentration, but the influence of homogenization cycle on particle size was not so dominant.

The interaction **term BC** i.e. with the increase in the homogenization pressure and increase in the homogenization cycles the particle size was found to be decreasing.

The value of correlation coefficient, R^2 for particle size was found to be 0.9913 which indicated good fit of the model.

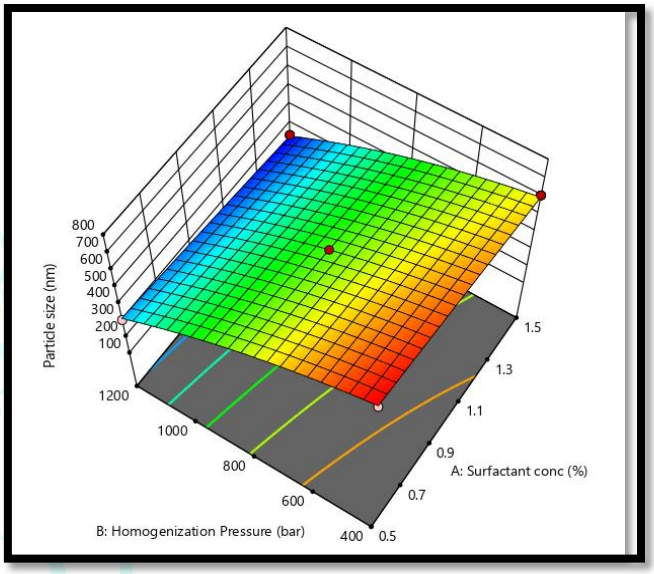


Figure 3: Response surface plot showing influence of concentration of surfactant and homogenization pressure on particle size.

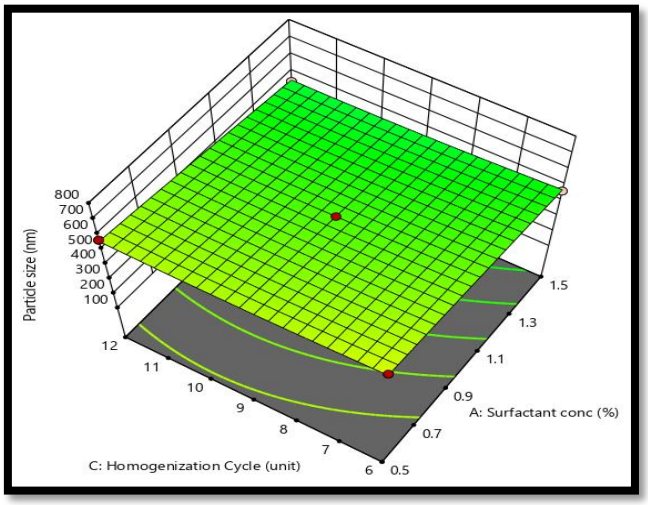


Figure 4: Response surface plot showing influence of concentration of surfactant and homogenization cycle on Particle size.

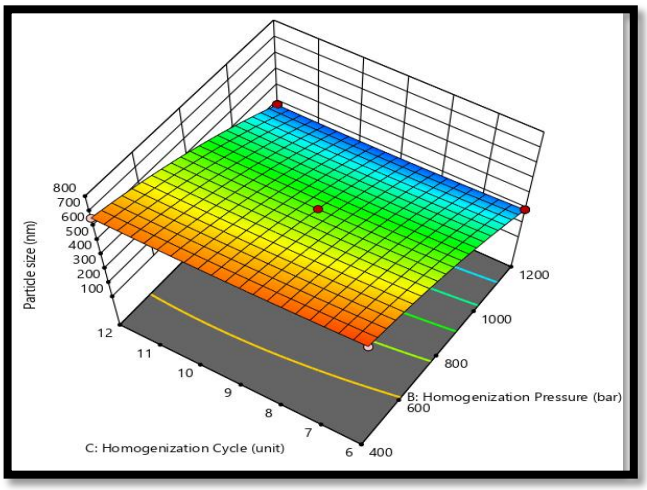


Figure 5: Response surface plot showing influence of homogenization pressure and homogenization cycle on Particle size.

3.6.2 Determination of Entrapment Efficiency:

The %EE is the amount of drug trapped in SLN as against the amount which was added to the process. The %EE was found to range between 70 - 92.33%. There was a linear relation between all the factors and the decrease in entrapment.

Equation 4 for Entrapment Efficiency:

$$\text{Entrapment Efficiency} = +89.00 - 7.87\,A - 3.61\,B - 0.7938\,C - 2.37\,AB - 1.33\,AC + 0.1250\,BC - 3.65A^2 - 1.81B^2 - 0.6063\,C^2$$

The model indicates that as the **term A** (concentration of tween 80) goes on decreasing the drug incorporation ability increases and thus the entrapment efficiency increases Equation (4).The high surfactant concentration causes large decrease in particle size and thus high interface for transfer of entrapped drug to dispersion medium resulting in decreased entrapment efficiency. The **term B** (homogenization pressure) had most dominant effect which is due to homogenizing valve under high density fluid-dynamic energy conditions. It was observed that entrapment efficiency was not significantly affected by the **Term C** (homogenization cycles) but increasing number of homogenization cycles decreased entrapment efficiency due to the aggregation of particles.

The **interaction term AC** i.e. the concentration of surfactant and homogenization cycle was seen to contribute reduction in drug entrapment which is because lower particle size of globules leading to enhanced area of migration of drug to aqueous phase.

The interaction term AB i.e. concentration of surfactant and homogenization pressure led to mild increase in the entrapment efficiency due to contribution of pressure.

The **interaction term BC** i.e. Entrapment efficiency was not highly affected by homogenization pressure and homogenization cycle. Similar effects were shown in figure 6 and 7.

The value of correlation coefficient, R^2 for Entrapment efficiency was found to be 0.9876 which indicated good fit of the model.

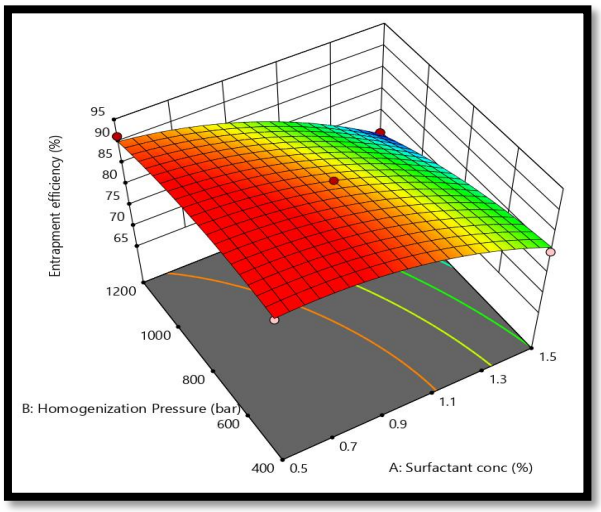


Figure 6: Response surface plot showing influence of concentration of surfactant and homogenization pressure on entrapment efficiency.

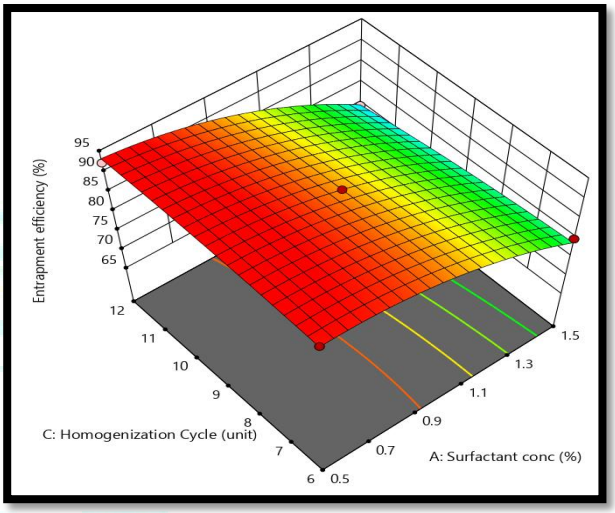


Figure 7: Response surface plot showing influence of concentration of surfactant and homogenization cycle on entrapment efficiency.

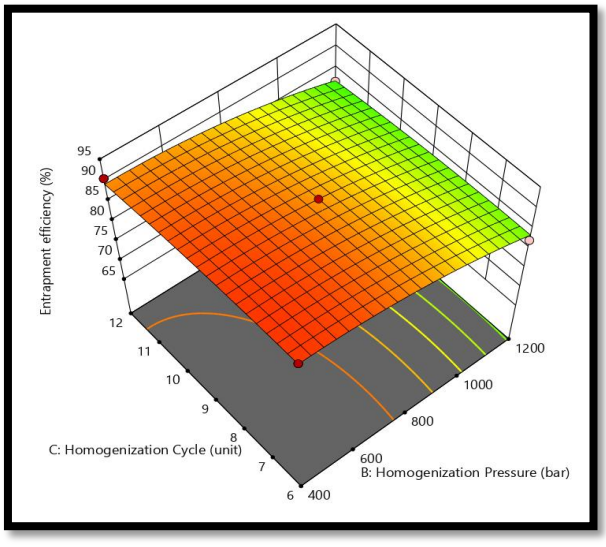


Figure 8: Response surface plot showing influence of homogenization pressure and homogenization cycle on entrapment efficiency.

The optimized batch was determined using desirability function, the criteria for optimization for particle size were to minimize and for EE it was to maximise. The solution obtained with highest desirability (0.98) was chosen which comprised 1% surfactant, homogenization pressure 1200 and homogenization cycles 9. To evaluate the findings, verification run was carried out and no significant difference was found between the theoretical and the actual values of particle size and entrapment efficiency (Table 7). Thus the proposed model was seen to have high prognostic ability.

Table 7: Check Points for optimization, actual, predicted value and % error (n=3, Mean± SD)

Formulation Code	Composition of optimized formulation			Response	Predicted Value	Actual Value	% Error
	X1	X2	X3				
OF9	1	1200	9	Y1	239.66 nm	237 nm	2.66
				Y2	93.26%	91.33%	1.93

The particle size of Blank SLN was found to be 200 nm. However, the zeta potential of Ginger extract solid lipid nanoparticles was seen to be slightly different to the Blank SLNs as seen in Table 8.

Table 8: The particle size, zeta potential and entrapment efficiency of Blank Solid Lipid Nanoparticles and ginger extract Solid Lipid Nanoparticles are given in table. (n=3, Mean± SD)

Formulation	Particle Size (nm)	Zeta Potential (mV)	Polydispersity Index	Entrapment Efficiency
Blank SLNs	200	-32.8	0.286	---
[6]GE-SLNs	237	-25.3	0.350	91.33

3.7 Differential Scanning Calorimetry (DSC):

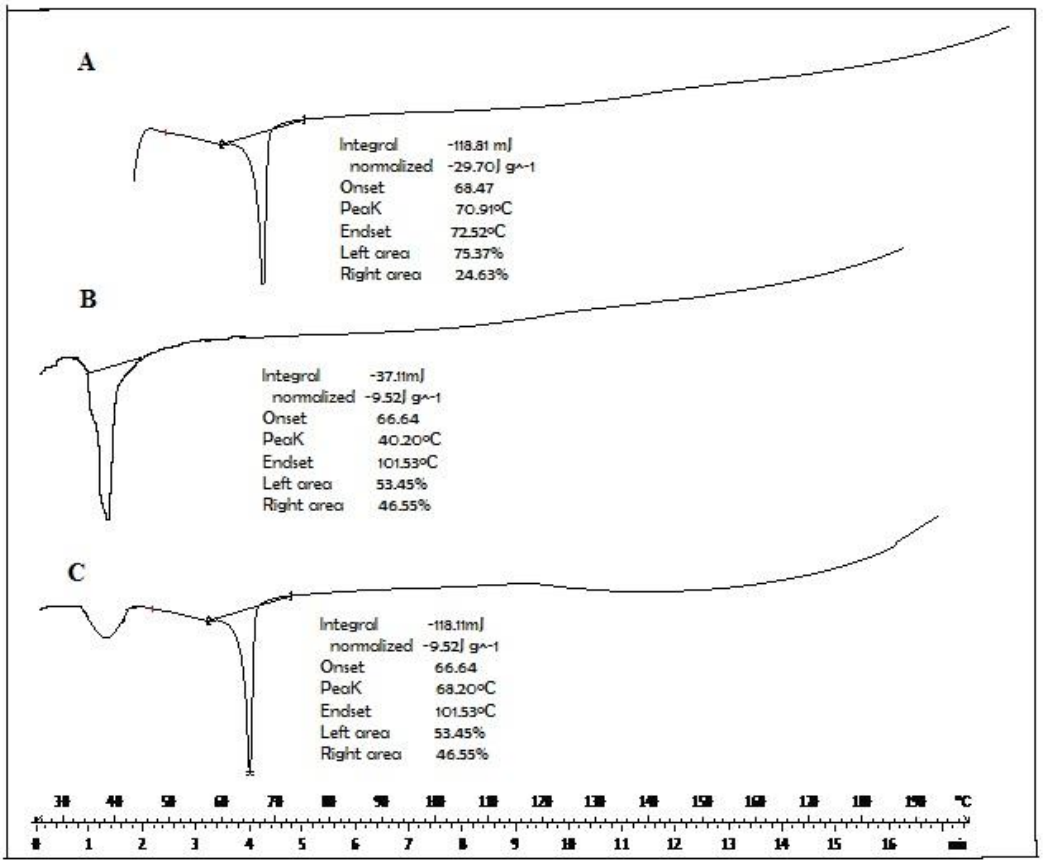


Figure 9: DSC thermograms of A]Stearic acid, B] (6)-Gingerol and C] (6)-Gingerol Solid Lipid Nanoparticles (GE-SLNs)

The melting endotherm of (6)-Gingerol and Stearic acid was observed at 40.20ºC and 70.91ºC respectively (Figure 8). The DSC thermograms of Solid Lipid Nanoparticles showed an endotherm at 68.20ºC this can be attributed to melting of Stearic acid in Solid Lipid Nanoparticles. This Shift of Solid Lipid Nanoparticles peak may be attributed to decrease in particle size and increase in the surface area. The endotherm of (6)-gingerol disappeared which indicates it is molecularly entrapped in stearic acid matrix.

3.8 Ex-vivo Studies:

The lymphatic uptake of nanoparticles involve numerous energy dependent processes of which primary are clathrin-mediated endocytosis (receptor-mediated process), caveolae-mediated endocytosis (receptor-mediated process) and clathrin-caveolae independent process[19]. To demonstrate the existence of cellular uptake pathways for SLN, the experiment was carried out in the presence of inhibitors of clathrin as well as caveolae mediated endocytosis. Chlorpromazine, a cationic, amphiphilic drug, is reported to inhibit clathrin-mediated endocytosis by causing accumulation of clathrin in late endosomes thus reducing its availability on the enterocytes surface. The caveolae are special type of lipid rafts rich in cholesterol and sphingo lipids that are flask- shaped invagination on the plasma membrane to engulf cargo molecules or carriers binding to their surface. Antifungal drug nystatin is known to block the caveolae mediated uptake by cholesterol sequestration [20,21,22].

Figure 9 represents the apparent permeability of the (A) SLN containing Ginger extract at 37 °C, (B) SLN containing Ginger extract at 4 °C, (C) In presence of Chlorpromazine at 37 °C and (D) In presence of Nystatin at 37 °C measured at 30 minutes. It was evident from the results that the apparent permeability in presence of Chlorpromazine was found to be 15.83%. Similarly, the apparent permeability in presence of Nystatin was also found to be reduced to 20.8%, thus concluding the contribution of both clathrin and caveolae mediated process in the uptake of Solid Lipid Nanoparticles. After application of single way ANOVA followed by Turkey's multiple comparison test, the difference between A, B, C, D was found significant ($p < 0.001$). The reduction in the apparent permeability at 4 °C to 8.2% in comparison with that at 37 °C also confirms the mechanism.

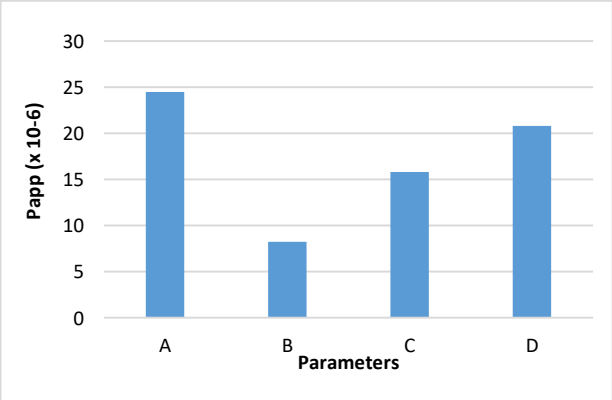


Figure 9: Ex-vivo apparent permeability of SLN containing Ginger extract at A) SLN at 37 °C B) SLN at 4 °C C) In presence of Chlorpromazine at 37°C, D) In Presence of Nystatin at 37°C

4. CONCLUSION:

The study investigated formulation optimization of DMARD (6)-Gingerol SLN for lymphatic uptake which can reduce side effects and improve concentration at inflamed site treatment of RA. The study through ex vivo study using everted rat gut sac model established that SLN containing Ginger extract with particle size **237** nm and zeta potential **-25.3** mV of (6)-Gingerol SLN can effectively be taken up by lymphatic route, as demonstrated by lack of uptake in presence of lymphatic uptake blockers.

Declaration of interest:

'Declarations of interest: none'.

Acknowledgements:

Authors are thankful to the Principal and Management of AISSMS College of Pharmacy, Pune for providing required facilities for research work and also thankful to "Research promotion Scheme" (RPS) for providing funding to this project.

REFERENCES:

1. Dr. Prakash D, Katiyar NS, Singh AP, Dr. Gangwar AK. Evaluation of anti-arthritic potential of zingiber officinale in expetimental rats. European Journal of Pharmaceutical and medical research 2016;3(4):305-308.
2. Rao J K, Mihaliak K, Kroenke K, Bradely J, Tierney W M, Weinberger M. Use of complementary therapies for arthritis among patients of rheumatologist. Annals of internal medicine 1999; 131(6):409-416.
3. Chang J M, Cheng CM, Hung LM, Chung YS, Rey YW. Potential use of plectranthus amboinicus in the treatment of rheumatoid arthritis. eCAM 2010;7(1)115–120.
4. Kaur A, Nain P, Nain J. Herbal plant used in rheumatoid arthritis: a review. International Journal of Pharmacy and Pharmaceutical Sciences 2012;4:44-57.
5. Wang Q,Wei Q,Yang Q,Cao X,Li Q,Shi F,Tong S,Feng C,Yu Q, Yu J, Xu X. A novel formulation of (6)-Gingerol: Proliposomes with enhanced oral bioavailability and antitumor effect. International Journal of Pharmaceutics 2017; 535(1):308-315.
6. Yang Xu, et al., Enhanced oral bioavailability of (6)-Gingerol-SMEDDS: Preparation, in vitro and in vivo evaluation. Journal of Functional Foods 2016; 27:703-710.
7. Bader R. The Development of Targeted Drug Delivery System for Rheumatoid Arthritis Treatment. Rheumatoid Arthritis-Treatment, Dr. Andrew Lemmey (Ed.), IntechOpen 2012; 978-953.
8. https://pubchem.ncbi.nlm.nih.gov/compound/gingerol/last accessed on 23/01/2019.
9. Müller H, Mäder K, Gohla S. Solid lipid nanoparticles (SLN) for controlled drug delivery-A review of the state of art. European Journal of Pharmaceutics and Biopharmaceutics. 2000; 50(1):161-177.
10. Bye W A, Allan J R, Trier. Structure, distribution and transport of preabsorbed origin of M cells in Peyer's patches of mouse ileum. Gastroentrology 1984; 86: 789-801.
11. Owen R L, Jones A L. Epithelial cell specialization within human Peyer's patches: an ultrastructural study of intestinal Lymphoid follicles. Gastroentrology 1974;66(2): 189-203.
12. Barthe L, Bessouet J. The improved everted Gut Sac: a simple method to study intestinal P-Glycoprotein, International Journal of Pharmaceutics 1998; 173(1-2): 225-258.
13. Rohit K, Ajage V, Kasture S. Validated UV spectroscopic method for the estimation of three marker compounds in marketed polyherbal ayurvedic formulation. Der Pharmacia Lettre 2014, 6 (3):160-166
14. Greenhalgh DJ, Willams AC, Solubility parameters as predictors of miscibility in solid dispersions. Journal of Pharmaceutical Science 1999; 88(11):1182–1190.
15. Fedors, R. A Method for Estimating both the Solubility Parameters and Molar Volumes of Liquids. Polymer Materials Science and Engineering 1974; 14 (2): 147-154.
16. Sacchetti M, Nejati E. Prediction of Drug solubility in lipid mixture from the modifying individual ingredient, APPS PharmSciTech 2013; 13(4): 1103-1109.
17. Gambhire M, Bhalekar M, Shrivastava B. Bioavailability assessment of simvastatin loaded solid lipid nanoparticles after

oral administration. Asian Journal of Pharmceutical Sciences 2011; 6(6): 251-258.
18. Mangesh Bhalekar, Prashant Upadhaya, Ashwini Madgulkar. Formulation and characterization of solid lipid nanoparticles for an anti-retroviral drug darunavir. Appl Nanosci 2017; 7:47–57
19. Lind M, Jacobsen J, Holm R, Müllertz A. Intestinal lymphatic transport of halofantrine in rats assessed using a chylomicron flow blocking approach: the influence of polysorbate 60 and 80. European Journal of Pharmaceutical Sciences 2008; 35(3):211–218.
20. Goyal S, Vashist H, Gupta A, Jindal S. Development of Alginate gel beads-entrapped liposomes for colon specific drug delivery of Prednisolone. Der Pharmacia Sinica 2011; 2(2): 31-38.
21. Barthe L, Woddley J, Houin G. Gastrointestinal absorbtion of drugs: method and studies. Fundamental Clinical Pharmacology 1999; 13(2): 154-168.
22. Sahay G, Alakhova D, Kabanov A. Endocytosis of nanomedicines. Journal of Controlled Release 2010; 145(3): 182-195.
23. Chimmiri P et al, Solid lipid nanoparticles: A novel carrier for cancer therapy. International Journal of Biological & Pharmaceutical Research 2012;3(3):405-413.
24. Pachuau L, Mazumder B. A study on the effects of different surfactants on Ethylcellulose microspheres. International Journal of PharmaTech Research 2009; 1(4): 966-971.
25. Gadhiri M, Vatanara A. Loading hydrophilic drug in solid lipid media as nanoparticles: Statistical modelling of entrapment efficiency and particle size. International Journal of Pharmaceutics 2012; 424(1-2): 128-137.
26. Li S, Ji Z, Zou M. Preparation, Characterization, Pharmacokinetics and Tissue Distribution of Solid Lipid Nannoparticles Loaded with Tetrandrine. APPS PharmSciTech 2011; 12(3): 1011-1018.
27. Roger E, Lagarce F, Garcion E, Benoit J. Biopharmaceutical parameters to consider in order to alter the fate of nanocarriers after oral delivery. Nanomedicine (London) 2010; 5(2): 287-306.

Journal of Drug Delivery & Therapeutics
JDDT